High speed sub-micrometric microscopy using optical polymer microlens

X. H. Zeng (曾新华)[1,2*], J. Plain[1], S. Jradi[1], P. Renaud Goud[1], R. Deturche[1], P. Royer[1], and R. Bachelot[1]

[1] *Laboratoire de Nanotechnologie et d'Instrumentation Optique, ICD CNRS FRE 2848, Université de technologie de Troyes, 12, rue Marie Curie, 10010 Troyes, France*

[2] *Department of Physics, Shanghai Jiao Tong University, Shanghai 200030, China*

[*] *E-mail: xinhua.zeng@utt.fr*

Received July 14, 2009

We report the high speed scanning submicronic microscopy (SSM) using a low cost polymer microlens integrated at the extremity of an optical fiber. These microlenses are fabricated by a free-radical photopolymerization method. Using a polymer microlens with a radius of curvature of 250 nm, a sub-micrometric gold pattern is imaged experimentally by SSM. Different distances between the tip and the sample are used with a high scanning speed of 200 cm/s. In particular, metallic absorption contrasts are described with an optical spatial resolution of 250 nm at the wavelength of 532 nm. Moreover, finite-difference time-domain (FDTD) simulations concerning the focal lengths of microlenses with different geometries and heights support the experimental data.

OCIS codes: 130.0130, 160.0160, 180.0180.

doi: 10.3788/COL20090710.0901.

The ability of rapid fabrication of a microlens at a fiber end in a cheap way enables a variety of applications for optical functional devices, such as couplers and collimators for waveguides or photonic crystal fiber (PCF) lasers[1,2]. Integrating microlens at the extremity of an optical fiber end enables the coupling of high power laser beam and strong light confinement.

In spite of the promising applications of microlens or microtip integrated at fiber end, manufacturing a microlens at the extremity of a fiber is a complex work. During the past decades, numerous efforts have been made by a variety of research groups to address this issue. The most available method is so-called mechanical pulling method or melt-stretched etching method[3,4]. The advantage of this method is that a small probe radius may be obtained. Nevertheless, this advantage is overpassed by its main limitation, which is a poor optical transmission efficiency of the order of 10^{-6}[4]. Low reproducibility and uncontrollability of the probe end shape are other obstacles for its fabrication. Another mostly mentioned method is the chemical etching, which allows the fabrication of tips with roughly the same poor characteristics[5,6]. Matsumoto *et al.* have developed a method to fabricate a near field optical fiber probe with nanometric metallized protrusion[7]. A high optical transmission efficiency of about 5% is reported. Nevertheless, the preparation process is relatively complex and not easy for the manufacturing in large scale. In this letter, we present simple and convenient route for the fabrication of sub-200-nm polymer probes with symmetric end shapes integrated at the end of a monomode fiber. Geometry of the tip, simulation of the electromagnetic field at the extremity of the tip, and imaging experiments are presented.

The basic principle of free-radical photopolymerization method is presented in detail in Refs. [8] and [9]. In this work, eosin Y (2',4',5',7'-tetrabromofluorescein disodium salt), methyldiethanolamine (MDEA), and pentaerythritol triacrylate (PETIA) are used as photosensitive dye, cosynergist, and multifunctional monomer, respectively. The multifunctional acrylate monomer of PETIA is used as a solvent. 4 wt.-% MDEA and 0.5 wt.-% eosin Y are added into the solvent in succession.

The formulation is highly sensitive in the spectral region from 450 to 550 nm. Therefore, it becomes photo polymerizable by the irradiation of an argon ion laser (514 or 488 nm), a frequency-doubled Nd:YAG laser (532 nm), or a green He-Ne laser (543.5 nm). Typically, a frequency-doubled Nd:YAG laser is suitable for this system and it is used in the probe fabrication. Firstly, a droplet of photosensitive formulation was deposited on a well-cleaved single-mode optical fiber top end. Subsequently, a laser beam (λ=532 nm) coupled from the other fiber end polymerized the monomer within the formulation. Resulting from the emerging Gaussian light beam, a tiny polymer lens formed at the beginning of the process. This tiny lens confined the light and permitted the consecutive polymerization to be oriented. The polymer acted as a guide and finally formed a cross-linked polymer microlens or microtip. After irradiation, unpolymerized monomers were removed using ethanol. As shown by the scanning electron microscopic (SEM) images in Fig. 1, the polymer probe fabricated by this method can be tunable between less than 1 μm to 300 μm in length and a curvature radius from several microns to several tens of nanometers by adjusting the photonic conditions of fabrication including exposure intensity and exposure time, and a smart dipping (for the long probe) or wipe-off technique (for the short one), which will be discussed in detail elsewhere. We controlled the curvature radius with reproducibility better than 90%. The length of the long polymer tips is somehow difficult to control exactly,

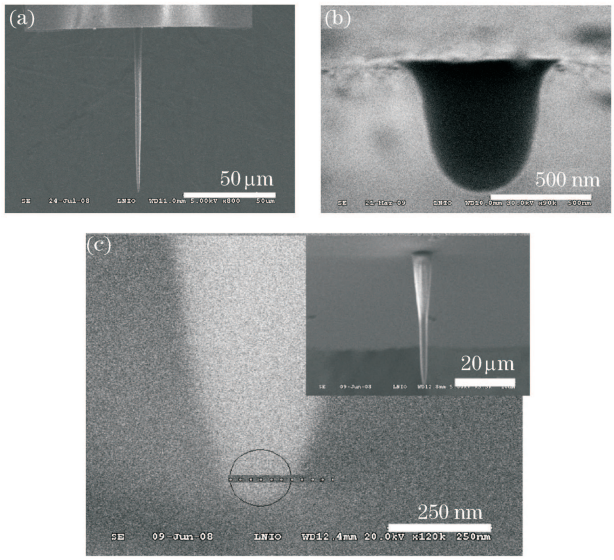

Fig. 1. SEM images showing polymer microlenses with different lengths and geometries. (a) Polymer microtip with an approximate length of about 100 μm fabricated by an exposure intensity of 250 nW for 2 s; (b) polymer microlens 700 nm in length and 500 nm in curvature radius fabricated with a smart shape control of formulation droplet; (c) polymer microtip with a typical length of 30 μm and a fine curvature radius inferior to 75 nm.

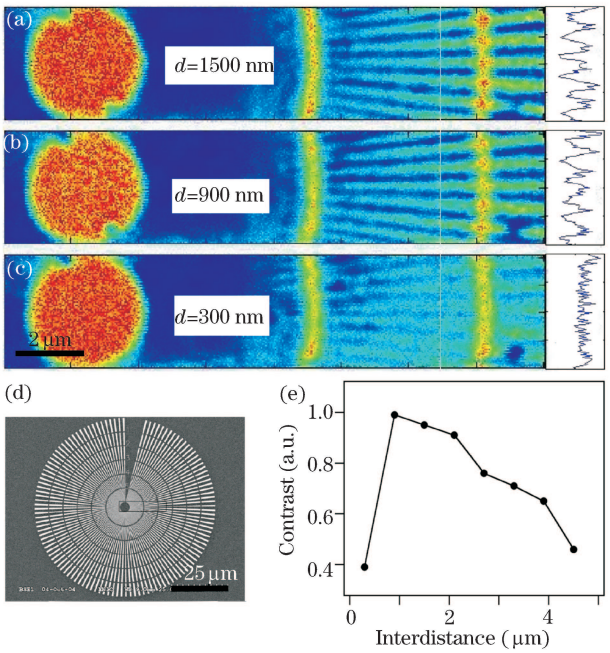

Fig. 2. Optical images of one part of a gold umbrella framework observed experimentally with tip-sample distances of about (a) 1500 nm, (b) 900 nm, and (c) 300 nm. The profiles correspond to white lines in the left images. (d) SEM image representing the gold "Japanese umbrella" sample. (e) Contrast measured on the profiles as a function of the distance tip-sample.

whereas the length of the short ones can be well controlled with a deviation lower than 3%. Moreover, a very high transmission efficiency was detected for this kind of polymer tips. Indeed, losses have been measured to be about 0.31 dB.

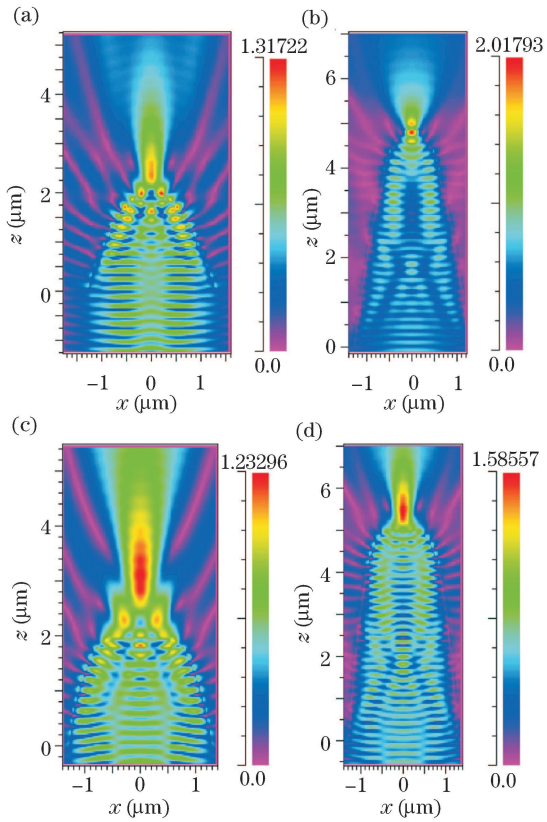

Fig. 3. Two-dimensional FDTD simulation results for polymer microlens with (a) α=2 and h_0= 2 μm, (b) α=2 and h_0= 5 μm, (c) α=4 and h_0= 2 μm, and (d) α=4 and h_0=5 μm. Refractive indices of 1.52, 1.47, and 1.4652 are assumed for the polymer, optical fiber core, and fiber cladding, respectively.

The polymer microlens is very promising as probe for far/near field sub-micrometric microscopy. We have developed a high speed sub-micrometric microscope using this kind of optical polymer microlens that permits a high scanning speed of 200 cm/s. Optical images in transmission and reflection mode can be achieved simultaneously. Here we only show the results of optical images in transmission for a sub-micrometric gold sample of "Japanese umbrella framework", as shown in Fig. 2(d). The black dashed rectangle illustrates the selected scanning area for the experiment. The polymer microlens was approached to the sample with a z-step of 30 nm. An optical image can be obtained for every z-step or every several z-steps as programmed. The images were recorded with a scanning speed of 200 cm/s and the scanning steps for both x and y axes for the recorded images are 50 nm. Selected images with tip-sample distances of 1500, 900, and 300 nm are shown in Figs. 2(a)−(c), respectively. The profiles have been measured on the white line in the different images. Gold features are about 250 nm in width for the considered profiles. In Fig. 2(e), the corresponding calculated contrast is given as a function of the distance tip-sample. The contrast C is calculated as

$$C(y) = 2 \times \frac{y_{\max} - y_{\min}}{y_{\max} + y_{\min}}, \quad (1)$$

where y stands for the measured signal received by the charge-coupled device (CCD). It clearly appears that the

best contrast is obtained for a distance tip-sample of about 1 μm that should be considered as the focal length of the microlens.

To illustrate the polymer microlens' optical properties, such as its focal length, a finite-difference time-domain (FDTD) simulation was performed. We generally define the taper-structured polymer microlens as

$$z = F(x) = h_0(\frac{w_0 - x}{w_0})^{\alpha}, \quad (2)$$

where h_0 is a constant defined as the height of the polymer tip; w_0 is the half width of the polymer lens on the base, namely, 1.3 μm for our case; and α is the taper shape factor. Typically, we assumed the refractive index of the polymer as 1.52, and 1.47 and 1.4652 for the optical fiber core and cladding, respectively. The diameter of the fiber core was assumed to be 2.6 μm. Simulation conditions are λ=532 nm, h_0=2 or 5 μm, and α=2 or 4. Typical simulation results are displayed in Fig. 3. A confined light field with full-width at half-maximum (FWHM) in the range of about 500 to 1200 nm is found. Moreover, the focal length is comprised between 0 (contact) to 1 μm with a field depth of about several hundred of nanometers to several microns. These typical results are in good agreement with the focal length and resolution measured experimentally.

In conclusion, polymer microlenses with different geometries, diameters, and heights have been integrated at a commercial optical fiber end by a free-radical polymerization. A test sample (gold nano umbrella) with a decreased line interdistance has been characterized experimentally using a polymer microlens for high speed sub-micrometric microscopy. The results have shown an optical spatial resolution of 250 nm at the wavelength of 532 nm. A promising effective technique for high-speed far/near field imaging at sub-micrometric scale is demonstrated.

X. H. Zeng thanks the CSC-UT/INSA Program for the PhD financial support.

References

1. R. Bachelot, C. Ecoffet, D. Deloeil, P. Royer, and D.-J. Lougnot, Appl. Opt. **40,** 5860 (2001).
2. J. P. Fillard, M. Castagne, and C. Prioleau, Appl. Opt. **34,** 3737 (1995).
3. H. L. Ren, C. Jiang, W. S. Hua, M. Y. Gao, J. Y. Wang, H. Wang, J. T. He, and E. J. Liang, Opt. Laser Technol. **39,** 1025 (2007).
4. R. C. Dunn, G. R. Holtom, L. Mets, and X. S. Xie, J. Phys. Chem. **98,** 3094 (1994).
5. R. Stokle, C. Fokas, and V. Deckert, Appl. Phys. Lett. **75,** 160 (1999).
6. P. Lambelet, A. Sayah, M. Pfeffer, C. Philipona, and F. Marquis-Weible, Appl. Opt. **37,** 7289 (1998).
7. T. Matsumoto, T. Ichimura, T. Yatsui, M. Kourogi, T. Saik, and M. Ohtsui, Opt. Rev. **5,** 369 (1998).
8. C. Ecoffet, A. Espanet, and D. J. Lougnot, Adv. Mater. **10,** 411 (1998).
9. A. Espanet, C. Ecoffet, and D. J. Lougnot, J. Polym. Sci. A: Polym. Chem. **3,** 2075 (1999).